

Modern Characterization Techniques for Functional Polymers



H. M. Fayzan Shakir and Rukhsar Anum

Abstract Polymers and their composites are preferred over conventional materials like steel, copper, and aluminum due to their high corrosion resistance, flexibility, ease of processability, and lightweight. Various analytical techniques have been used for the characterization of polymers and their composites as a function of either time or temperature. Morphological structure, molecular weight, analysis of monomer, solvent residue, the composition of the copolymer, and interfacial interfaces of polymeric systems are some of the advanced properties of polymers and composites. The current chapter covers some of the advanced characterizations techniques like Dynamic Mechanical Analysis (DMA), Thermomechanical Analysis (TMA), Atomic Force Microscopy (AFM), 4-Probe technique, Inverse Gas Chromatography (IGC), and Gel Permeation Chromatography (GPC). The above-mentioned techniques are used to determine various properties of advanced polymers like their response to heat, stress, electrical resistance, molecular weight, etc.

1 Introduction

An extensive range of analytical techniques has been established for polymer characterization and their composites across the time. Most of these techniques have been used for identifying the physical properties while some of these are used for determining the chemical structure. The polymers are characterized by these different techniques as either function of time or temperature. Thermo-analytical techniques are generally used for the identification of physical properties. Thermal analysis is an enormously diverse technique with a wide range of different methods. Thermomechanical Analysis (TMA) is a sensitive and ideal thermal analytical technique that provides information about thermal expansion, softening points, and phase changes

H. M. Fayzan Shakir (✉)

Department of Materials, School of Engineering and Technology, National Textile University, Faisalabad, Pakistan

e-mail: Fayzan.shakir@ntu.edu.pk

R. Anum

Department of Chemistry, University of Agriculture Faisalabad, Faisalabad, Pakistan

in polymers as a function of temperature. Dynamic Mechanical Analysis (DMA) is an analytical technique that provides insight into its chain structure and is used to characterize the interfacial interfaces of polymeric systems.

In recent years, the technique of chromatography is attaining fame in the characterization of polymers. Different techniques such as size exclusion chromatography, gel permeation chromatography, and high-performance chromatography are integral parts of polymer characterization. These are used for the determination of molecular weight, analysis of monomer, solvent residue, composition of the copolymer, etc. Another technique gaining importance in polymer analysis is inverse gas chromatography for the investigation of residual monomers and impurities in the polymer [1]. Some of the characterization techniques for the polymer are explained for better understanding.

2 Dynamic Mechanical Analysis

Dynamic mechanical analysis (DMA) is an analytical practice that provides insight into chain structure and inter-phase interaction in polymer blends. For complex materials like advanced polymer composites, during the DMA spectra interpretation, some attention is essential, especially while determining the glass transition temperature (T_g). For measuring the dynamic mechanical properties in filler-filled polymers, DMA could be considered as one of the standard equipment.

In the DMA experiment, at a given frequency and temperature, an oscillating force is functional to the test material while the response of the material to the applied force is measured [2]. Stress (σ) is the applied force on the sample and strain (γ) is the deformation in the sample. For viscoelastic samples like polymers, the response of material magnitude (i.e., deformation amplitude) to the oscillating force applied is moved through phase angle (δ) shown in Fig. 1. The $\tan \delta$, loss, and storage modulus for a free coating sample analyzed by DMA are shown in Fig. 2. The relation between strain and applied stress is created in the material, both the loss modulus (E'') as well as elastic storage modulus (E') are calculated. E'' exhibits the ability of sample to dissipate or lose energy and E' exhibits the capability of the test material to return or store energy. The relation among both factors is called damping and expressed as $\tan \delta \left(\delta = \frac{E''}{E'} \right)$.

Different techniques are used to deform the samples in DMA e.g., shear stress, tension, or parallel plate blending. The peak values of $\tan \delta$ are utilized to exhibit the inner friction of the polymeric chain quantitatively. With particular particle size, surface area, and filler's loading, the number of mobile chain segments becomes higher with the outstanding dispersion of filler material in the matrix than in a system with poor dispersion of the filler. Increased mobile chain segments enhanced the inner friction and loss modulus, giving a high peak value at T_g of $\tan \delta$. When the concentration of particles in the polymer increased, the peak value of $\tan \delta$ reduced because of an increase in interfacial interaction [3]. However, DMA results provide

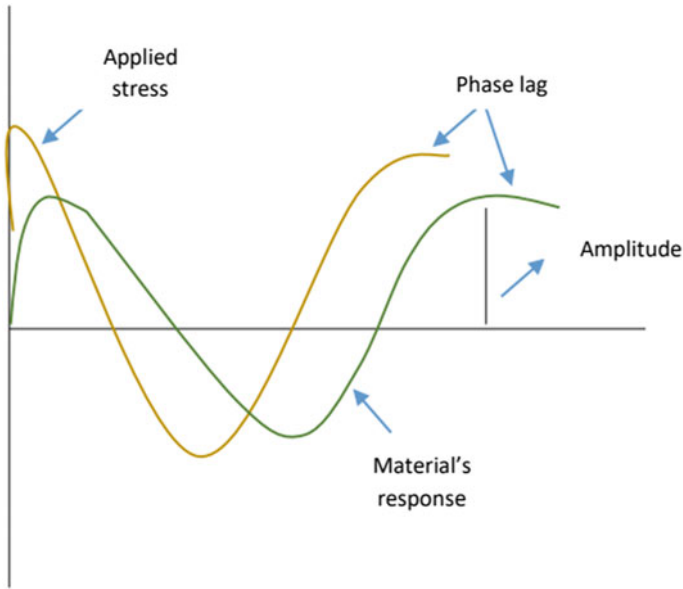


Fig. 1 Schematic illustration for applied stress to sample and response of sample in DMA

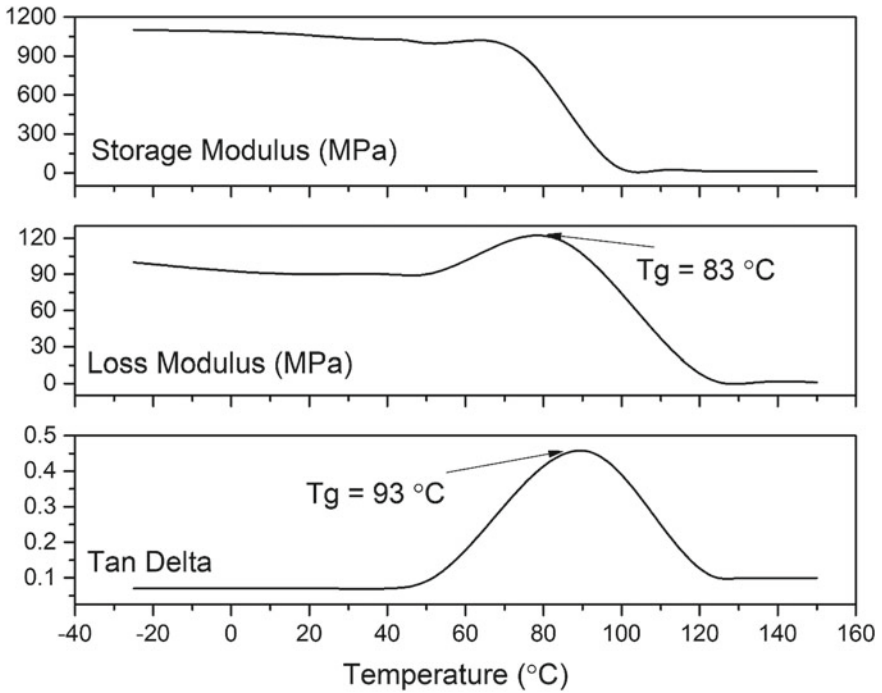


Fig. 2 Tan δ , loss and storage modulus results of a sample analyzed in DMA

useful information related to the extent of interfacial interaction in the region of interphase and the degree of dispersion of the fillers.

Eisenberg et al. [4] showed that the nanocomposites of silica with various polymers poly(methyl methacrylate), styrene-butadiene rubber (SBR), polystyrene (PS), polyvinyl acetate (PVA), and poly(dimethylsiloxane) (PDMS) could have two distinctive T_{gs} . DMA was used to examine the effect of silica nanoparticle content on several polymers. The T_g was estimated by the peak of the $\tan \delta$. The concentration of silica was varied from 0 to 50 wt% and all the filled composites exhibited two separate T_g s. The researchers recognized the first T_g as the majority of polymers and the second T_g accredited to the chain of polymers positioned in the interphase section of the composite. The interphase section consists of two nanolayers, the first nanolayer consists of the chains of polymer which are fixed due to the connection with the charged surface of particles while the next layer is thicker and formed away from the nanoparticle surface and consists of polymeric chains which are less bound to nanoparticles. With increased nanosilica content, the T_g location did not change but the $\tan \delta$ value decreased and this decrease is credited to the decrease in the polymer chain fraction that participates in the major conversion through increased silica amount in the composite. The second peak of $\tan \delta$ was wider and depending on the type of polymer was located about 40–110 °C high than that of the first one. The second T_g and second peak were reduced due to increased silica loading. The area below the two peaks of $\tan \delta$ reduced with silica content, i.e., at high filler content, $\tan \delta$ curve became thinner indicating lesser polymer chains participated in T_g . It was also suggested that with high filler loading >20 wt%, the polymer's volume fraction bound with the filler surface increased causing a reduction in the $\tan \delta$ curve width. It was also exhibited that the second T_g depends on the molecular weight and nature of the polymer and the nanofiller loading in the composite [5]. Further scientists [6, 7] presented that the major or inmost interfacial layer defines the T_g for composites.

3 Thermomechanical Analysis

Thermomechanical analysis (TMA) is a reliable, excellent, simple, sensitive, basic, and ideal thermal analytical technique. It provides information about softening points, T_g , phase changes, composition, and thermal expansion of materials having several geometries by applying the constant force as a temperature function. TMA is an elementary tool for polymer science because it can detect proficiently and precisely every probable transition and also dimensional change at the nano level [8]. The investigation study explained that the TMA technique can be efficiently utilized only or in combination with further TA techniques like DMA, TGA, or DSC because it is accurate and sensitive for recognizing T_g for polymers and polymer composite materials in contrast to traditional DSC. TMA is a highly sensitive analytical technique for the characterization of chemical and physical properties of polymers and composite materials that are unnoticeable [9]. The purpose of T_g from TMA, DMA, and DSC procedures are comparatively shown in Fig. 3. Extraordinarily, T_g for the

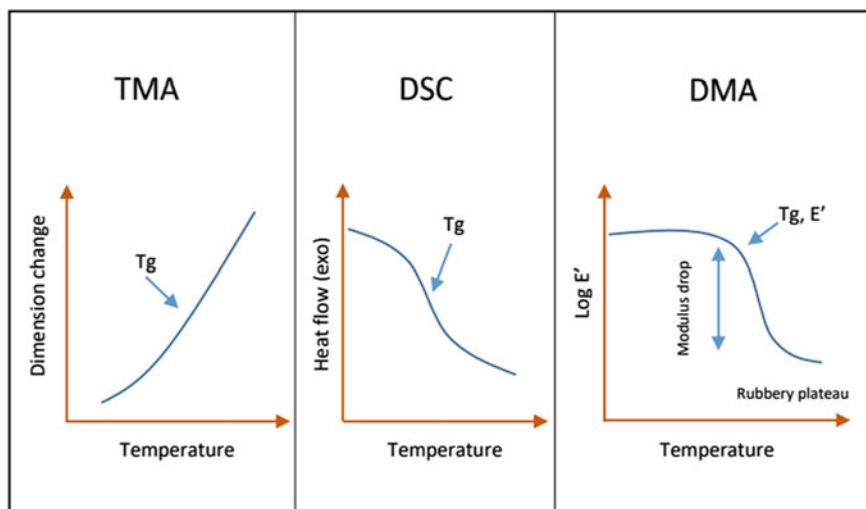
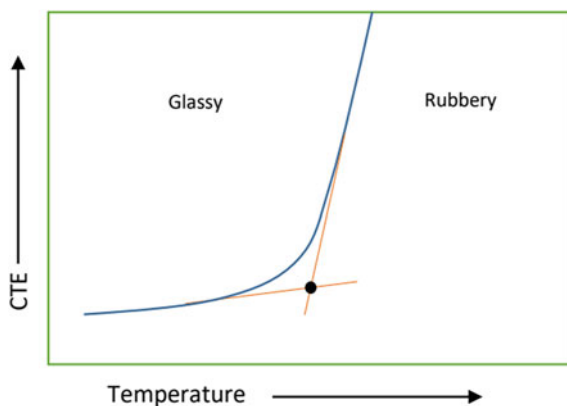


Fig. 3 Comparison of T_g from TMA, DSC, and DMA techniques

sample could be attained from the CTE curve, i.e., TMA graph by detecting the two curves of intercept plot among displacement versus temperature shown in Fig. 4.

TMA plot is efficiently utilized to explore T_g for polymers or polymeric nanocomposites as a polymer changes from a glassy state to rubbery through a modification in permitted molecular volume regarding CTE alteration as a function of pressure at temperature constant or a function of temperature at constant pressure [10]. The thermo mechanical characteristics of basalt fiber (BF) filled high-density polyethylene (HDPE) and co-extruded wood plastic composite with the composite shell of HDPE/BF were investigated. It was reported that the introduction of BF in HDPE

Fig. 4 T_g plot from TMA technique



reduced CTE for pure HDPE [11]. The thermal expansion behavior of nanocomposites was analyzed by the introduction of graphene sheets and graphene foam into polydimethylsiloxane (PDMS). It was detected that the graphene sheet/PDMS composite exhibited higher CTE than the composite of graphene foam/PDMS. Researchers observed it as a promising and attractive material for use in photonic and electronic devices for thermal management [12]. Currently, the TMA technique offers applications in different areas such as electroplating, construction, food packaging, and aerospace industry [13].

4 Atomic Force Microscopy

Atomic Force Microscopy (AFM) has been extensively used to do inquiries into the crystallization of polymers due to its remarkable strength which makes it preferable for advanced studies. High-resolution technology allows the fundamental dimension scale of the lamellar polymeric crystal to be measured. The sample preparation technique is simple as it demands no metal coating and staining. AFM is non-destructive in several conditions. The images can be obtained during the melting and crystal growth that provide lamellar and sub-lamellar resolution with respect to time. AFM provides polymer crystallization with crystal melting, crystal growth, and crystal organization at the lamellar scale that represents structure progress and influence of kinetics at local conditions. It has several measuring modes with the addition of various functional semi-crystalline polymers [14].

A sharp tip is present in AFM which is attached to the cantilever beam that makes contact with the surface of the sample. There are several modes of the technique but 'contact mode' as well as 'tapping mode' are frequently used. The measurement of the force of attraction by deflection of the cantilever between the tip and surface is done in contact mode which is generally monitored with an optical lever. The deflection of the cantilever is adjusted by the height of the base through the feedback loop. The force acting on the tip of the cantilever is known as linear spring at set point. The constant deflection is sustained by regulating the location of the cantilever through the feedback loop during the scanning of the cantilever point by point above the surface of the sample. The control vertical signal is used to synthesize a topographic image of the surface. The contact mode maintaining the interface of the tip and sample that exerts the adjacent attractions on the sample with tip is quite great, generally destroying loosely or soft samples [15].

The cantilever of 'tapping mode' oscillate at its resonance frequency. The tip makes interaction with the sample surface damped the amplitude of the oscillation

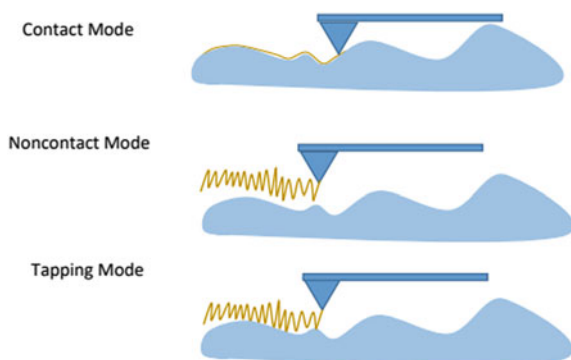
with the contact. The amplitude of oscillation is a constant value and is used as a feedback factor. The stable image of a soft sample of polymer can be obtained under the careful condition where the lateral forces are lesser than the contact mode of AFM. A set frequency driving the cantilever and contact with the properties of the material surface could be attained by observing the variance between the driven signal phase and the cantilever response phase—the phase image [16].

The excellent mode of technique is used to analyze the polymer crystal growth that has very sharp variations in the mechanical and adhesive characteristics among liquid and crystalline polymers. The monitoring of sample temperature is very necessary for the melting and crystallization of the polymers. The process of the stable and constant temperature of AFM has allowed an extensive range of polymers to attain images at the temperature of 0–250 °C during crystallization. The polymers susceptible to hydrolysis and oxidation are studied at high temperatures by use of an inert gas atmosphere and vacuum for environmental control. The crystallization of many polymers in AFM is allowed at the temperature range near T_g or T_m when the growth of the crystal is low [17] (Fig. 5).

Recently, an advanced form of AFM is developed that permits images to be composed at video rate and is known as Video-AFM. This advanced technology helps in understanding some progress for the growth of crystal but is troubled due to large tip-sample forces because Video-AFM needs constant tip-sample contact. The rate of at least 1 frame is needed for the recurrent contact mode image in the future advancement of this technique because fast scanning helps to understand the significant impact on our understanding of polymeric crystal growth in various varieties of systems.

Atomic force microscopy is an old technique and is advancing constantly with high-speed scanning, high-resolution imaging, and process of material mapping that are potentially important for the future applications of AFM to polymer crystal [18] (Fig. 6).

Fig. 5 Different modes of AFM



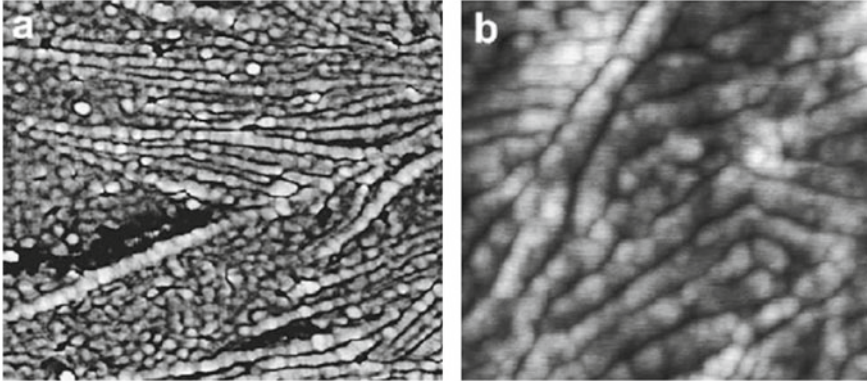


Fig. 6 AFM phase images of semi-crystalline polymer surface representing the observed ‘knobby’ substructure that has been thought due to its early crystallization in discrete blocks. Scale bars show 200 nm in **a** and 100 nm in **b** [19].

5 Probe Technique

The 4-probe technique is used to measure the conductivity of polymer materials. It can measure the conductivity of the material in either film or bulk. The instrument consists of equally sized tungsten metal tips with a fixed radius. Every strip is sustained by a spring on the other edge to reduce the damage to testing material during probing. All the metal tips are part of the auto-mechanical step which moves up and down during the process. The outer two probes provide the current by high impedance current source while the inner two probes determine the voltage through a voltmeter for measuring the resistivity of the sample polymer (Fig. 7).

The resistance is directly proportional to the length and inversely proportional to the area of the cross section of testing material at a constant temperature.

$$R = R = \rho L/A \quad (1)$$

ρ represents the resistivity of the conducting material and is measured in an ohm-meter.

$$\sigma = 1/\rho \quad (2)$$

Conductivity is reciprocal to resistivity and its temperature dependence is given by

$$\rho = A \exp \frac{E_g}{2KT} \quad (3)$$

E_g represents the band gap of the material, T represents the temperature in kelvin, and K represents the Boltzmann constant (8.6×10^{-5} eV/K).

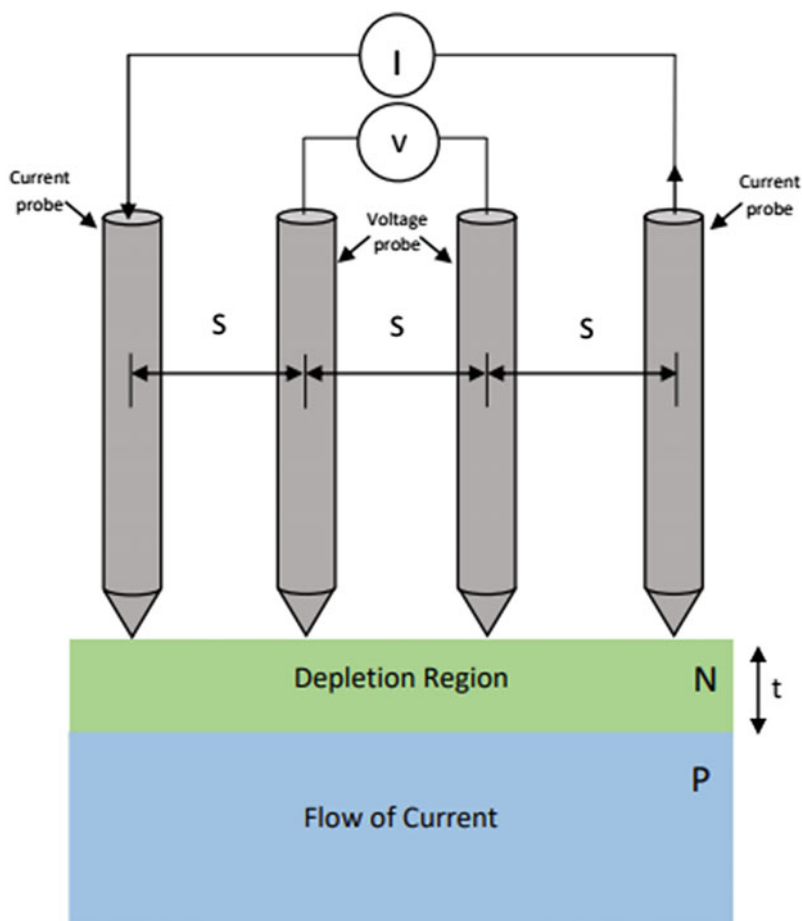


Fig. 7 4-probe technique

Yamanaka et al. measured the electrical conductivity of 3D polymer with dimensions of $0.2 \times 0.2 \text{ mm}^3$ at temperature range of 4–300 K by 4-probe technique [20]. Vas and Thomas also measured the electrical conductance of polymeric composite with increasing nanofiller of MWCNT by using 4-probe technique as shown in Fig. 8. Agilent device analyzer B1500A was used for these measurements.

6 Inverse Gas Chromatography

IGC is an accurate, fast, and reliable system for the physiochemical characterization of polymers, and their composites. The word 'inverse' represents the sample material

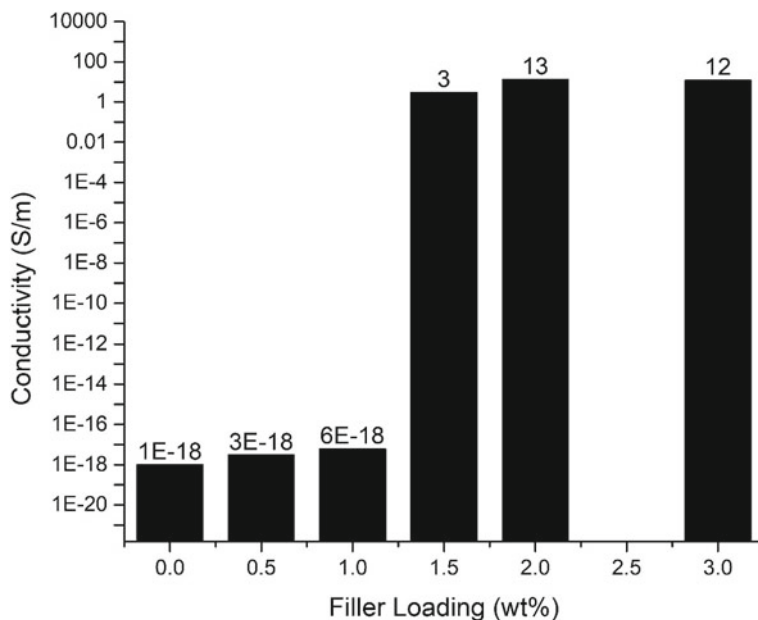


Fig. 8 Conductivity measurements for polymeric composite with nanofiller loading [21]

such as a polymer composite is a material of interest existing in the chromatographic column, in comparison to general analytical gas chromatographic experiments. The sample solute is carefully selected and injected into the tube of the carrier gas flowing over the surface of the sample. The peak elution and retention time of selected solutes are used to analyze the interactions that are affected by the contacts among the stationary phase and solutes.

The investigation of surface properties by this technique is quite interesting. Surface properties are commonly characterized by the use of factors that describe the ability of the surface to experience dispersive and acid-base characteristics. Free energy of the surface has a dispersive component of γ_s^d and specific interaction factors counting the ability of the surface to behave as a donor or acceptor are utilized for measuring the characteristics of polymeric surfaces [22] (Fig. 9).

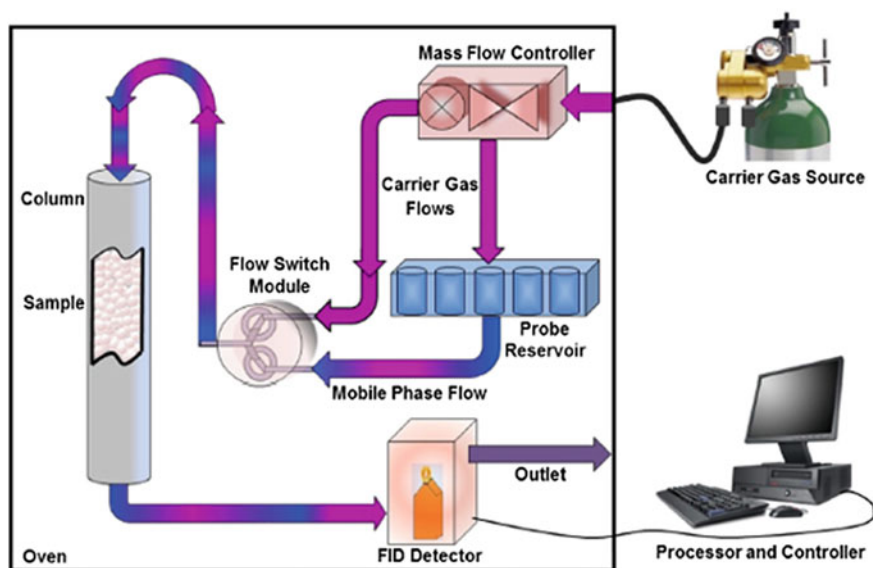


Fig. 9 Schematic representation of inverse gas chromatography analysis[23]

The dispersive component can be measured from Eq. (4) with experimentally determined value of ΔG_{CH_2} .

$$\gamma_s^d = \frac{\Delta G_{CH_2}}{4(6.023 \times 10^{23})^2 a_{CH_2}^2 \gamma_{CH_2}} \quad (4)$$

While

$$\Delta G_{CH_2} = -RT \ln \left(\frac{V_{N,n}}{V_{N,n+1}} \right) \quad (5)$$

$V_{N,n}$ and $V_{N,n+1}$ represents the net volume retentions of alkanes having n and $n + 1$ atoms respectively, a_{CH_2} represents the surface covered by polymer sample and γ_{CH_2} represents the free surface energy of the polymer.

Schultz et al. proposed the calculation of γ_s^d from the following equation:

$$RT \ln V_N = 2N(\gamma_s^d)^{1/2} a_p (\gamma_L^d)^{1/2} + c \quad (6)$$

a_p represents the occupied area by the adsorbing molecule of test material, γ_L^d is the dispersive component of adsorbent energy of the free surface, and c is constant. The technique is based on the linear relationship of ΔG^o and $a_p (\gamma_L^d)^{1/2}$ of alkanes and determination of γ_s^d from slop value.

Various restrictions for this technique have been indicated by Brendle and Papirer. The problems arose due to the proper determination of $a_p(\gamma_L^d)^{1/2}$ value, i.e., accurate measurement of inverse gas chromatography. The value of γ_s^d may be influenced by the different parameters such as applying reference state in the process and impact of bulk retention during porous polymer having temperature near to T_g or when a sample solute is utilized as solubilizer and solvent for polymeric sample. For reducing these problems, it must guide that the porosity of the sample polymer should be checked for its influence on the retention factor of sample solute and exertion at the temperature distance. These errors depend on the quality of determination of the slope value in the finding of dispersive components for the free energy of the surface in Eq. (6). Generally, the low value of the slope is multiplied by a constant value greater than three orders. The 10% error in the slope value results in the 20% inaccuracy in the γ_s^d values.

The experimental value of V_g and T can be determined accurately. The value of $a\gamma_L^d$ can be found from the experiment or can be collected from the literature. The main difficulty is finding the value of a_p that can be a larger error depending on the temperature, properties of the adsorbent as well as reference material. Its value can be obtained with one of these assumptions: (1) the test material may act as an ideal gas; (2) the value of a_p is constant; (3) at a temperature below the boiling point the test material act as real gas; (4) the test material act as a liquid when the adsorption depends on the density of the test material. Different models for the temperature dependence of a_p are present but these assumptions cannot complete the conditions of outcomes. The constant value of a_p is a most suitable assumption but in inverse gas chromatography, the behavior of test material as ideal gas seems to be realistic.

The significance of using IGC can be summarized as follows: (1) these are promising in checking the effect of modified arrangement on estimated factors and additional characteristics of sample materials; (2) this technique allows the examination of various porous polymers that have hardly determined surface activity, e.g., measurement of contact angle; (3) evaluation of the relationship between the surface properties and monolayer; (4) test of the effect of IGC experiment temperature on the surface is possible; (5) the alteration of surface properties may occur as the outcome of surface modification [24].

7 Gel Permeation Chromatography

Gel permeation chromatography (GPC) or size exclusion chromatography (SEC) having a refraction index as well as a viscosity detector is most important to attain information regarding the molecular weight of polymers. This technique is fast and runs more routinely in comparison to ^{13}C NMR. When joined with multidetector allows attaining detailed as well as fast characterization since different involved techniques give structural data which are attained instantaneously with standard GPC analysis. Suarez et al. [25] characterized the synthesized copolymers using the

GPC-4D technique by coupling GPC with four detectors: a viscometer, a refractive index, an infrared, and a multi-angle light scattering (MALS) detector.

The chromatography of gel permeation is Water Alliance 2000 having standard viscosity and refractive index detectors. In GPC, the separation was done by two columns, the flow rate was mLmin^{-1} , and the temperature was fixed at $145\text{ }^{\circ}\text{C}$. The solvent 1,2,4-trichlorobenzene (TCB) was added for stabilizing the polymer in opposition to oxidative degradation.

MALS detector was equipped at 690 nm with a laser and 17 multi-angle detectors. The temperature was $145\text{ }^{\circ}\text{C}$ and the joining between the MALS cell and GPC was carried out by using the heated line. Toluene was used for the calibration of the DAWN EOS system and the normalization of detectors was done using the polystyrene (PS) standard. Wyatt Technology software was used for the acquisition of online data and calculation of the average and distribution of the radius of gyration and molecular weight.

An infrared detector (IR) is a polymeric char detector joined with GPC by a heated transfer line at a temperature of $145\text{ }^{\circ}\text{C}$. It gives different wavelengths analysis equivalent to absorption at several IR bands which helps attain the intensity for the characteristic peaks of CH and CH_3 .

Homo and copolymers using several catalysts were fabricated covering a 0–50 mol% composition range of ethylene. For metallocene copolymers, with ethylene percentage, the molecular weight was decreased which was because of polymer crystallinity. For the Ziegler-Natta catalyst, the average molecular weight was high, and not a clear trend was seen with the copolymer composition. Classic results attained using the GPC-4D system are shown in Fig. 5. The molecular weight as well as molecular weight distribution (MWD) for every GPC slice is attained through a universal calibration curve by viscosity and refractive index detectors. Comonomer content attained through IR and the radius of gyration for every molecular weight slice attained through MALS are displayed. The comonomer distribution attained for copolymers is like that determined through the IR5-MCT detector [26], which confirmed the GPC-4D technique's accuracy. Therefore, it is promising to obtain broad information regarding comonomer distribution, molecular weight, and copolymer confirmation in solution [27] (Fig. 10).

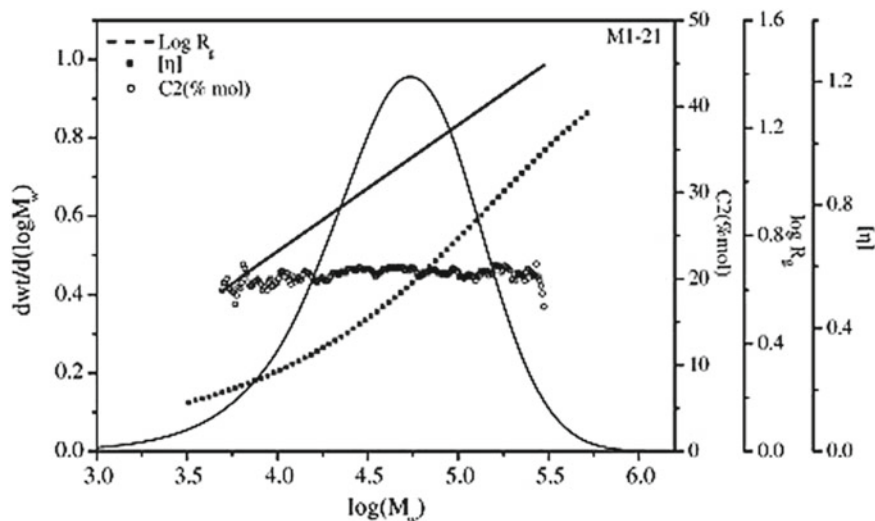


Fig. 10 Distribution of ethylene content, MWD, intrinsic viscosity, and radius of gyration for copolymers by GPC-4D technique

References

1. Van Lieshout, M.H.P.M., Janssen, H.G., Cramers, C.A., Hetem, M.J.J., Schalk, H.J.P.: Characterization of polymers by multi-step thermal desorption/programmed pyrolysis gas chromatography using a high temperature PTV injector. *HRC J. High Resolut. Chromatogr.* **19**, 193–199 (1996). <https://doi.org/10.1002/jhrc.1240190404>
2. Liang, J.Z.: Dynamic mechanical properties and characterization of inorganic particulate-filled polymer composites. *J. Thermoplast. Compos. Mater.* **24**, 207–220 (2011). <https://doi.org/10.1177/0892705710387254>
3. Bashir, M.A., Jakobsen, M.G., Farstad, V.B.: The effect of extender particle size on the glass transition temperature of model epoxy coatings. *Polymers (Basel)* **12** (2020). <https://doi.org/10.3390/polym12010196>
4. Tsagaropoulos, G., Eisenberg, A.: Dynamic mechanical study of the factors affecting the two glass transition behavior of filled polymers. Similarities Differ. *Random Lonomers, Macromol.* **28**, 6067–6077 (1995). <https://doi.org/10.1021/ma00122a011>
5. Bashir, M.A.: Use of Dynamic Mechanical Analysis (DMA) for characterizing interfacial interactions in filled polymers. *Solids.* **2**, 108–120 (2021). <https://doi.org/10.3390/solids2010006>
6. Mayes, A.M.: Softer at the boundary taking lessons from the book. *Nature* **4**, 651–652 (2005)
7. Starr, F.W., Schröder, T.B., Glotzer, S.C.: Effects of a nanoscopic filler on the structure and dynamics of a simulated polymer melt and the relationship to ultrathin films. *Phys. Rev. E Stat. Physics, Plasmas, Fluids, Relat. Interdiscip. Top.* **64**(5) (2001). <https://doi.org/10.1103/PhysRevE.64.021802>
8. Gaisford, S., Kett, V., Haines, P.: Principles of thermal analysis and calorimetry. Roy. Soc. Chem. (2019)
9. James, J.: Chapter 7—thermomechanical analysis and its applications. In: Thomas, S., Thomas, R., Zachariah, A.K., Mishra, R.K. (eds.) *Thermal and Rheological Measurement Techniques for Nanomaterials Characterization*, pp. 159–171. Elsevier (2017). <https://doi.org/10.1016/B978-0-323-46139-9.00007-4>

10. Corcione, C.E., Frigione, M.: Characterization of nanocomposites by thermal analysis. *Materials* (Basel). **5**, 2960–2980 (2012). <https://doi.org/10.3390/ma5122960>
11. Wu, Q., Chi, K., Wu, Y., Lee, S.: Mechanical, thermal expansion, and flammability properties of co-extruded wood polymer composites with basalt fiber reinforced shells. *Mater. Des.* **60**, 334–342 (2014). <https://doi.org/10.1016/j.matdes.2014.04.010>
12. Zhao, Y.-H., Wu, Z.-K., Bai, S.-L.: Study on thermal properties of graphene foam/graphene sheets filled polymer composites. *Compos. Part A Appl. Sci. Manuf.* **72**, 200–206 (2015). <https://doi.org/10.1016/j.compositesa.2015.02.011>
13. Saba, N., Jawaid, M.: A review on thermomechanical properties of polymers and fibers reinforced polymer composites. *J. Ind. Eng. Chem.* **67**, 1–11 (2018). <https://doi.org/10.1016/j.jiec.2018.06.018>
14. Balzano, L., Kukalyekar, N., Rastogi, S., Peters, G.W.M., Chadwick, J.C.: Crystallization and dissolution of flow-induced precursors. *Phys. Rev. Lett.* **100**, 1–4 (2008). <https://doi.org/10.1103/PhysRevLett.100.048302>
15. Hsiao, B.S., Yang, L., Somani, R.H., Avila-Orta, C.A., Zhu, L.: Unexpected Shish-Kebab structure in a sheared polyethylene melt. *Phys. Rev. Lett.* **94**, 1–4 (2005). <https://doi.org/10.1103/PhysRevLett.94.117802>
16. Klinov, D., Magonov, S.: True molecular resolution in tapping-mode atomic force microscopy with high-resolution probes. *Appl. Phys. Lett.* **84**, 2697–2699 (2004). <https://doi.org/10.1063/1.1697629>
17. Yang, X., Loos, J.: Toward high-performance polymer solar cells: the importance of morphology control. *Macromolecules* **40**, 1353–1362 (2007). <https://doi.org/10.1021/ma0618732>
18. Garcia, R., Proksch, R.: Nanomechanical mapping of soft matter by bimodal force microscopy. *Eur. Polym. J.* **49**, 1897–1906 (2013). <https://doi.org/10.1016/j.eurpolymj.2013.03.037>
19. Hobbs, J.K., Farrance, O.E., Kailas, L.: How atomic force microscopy has contributed to our understanding of polymer crystallization. *Polymer* (Guildf). **50**, 4281–4292 (2009). <https://doi.org/10.1016/j.polymer.2009.06.021>
20. Yamanaka, S., Kubo, A., Inumaru, K., Komaguchi, K., Kini, N.S., Inoue, T., Irifune, T.: Electron conductive three-dimensional polymer of cuboidal C60. *Phys. Rev. Lett.* **96**, 1–4 (2006). <https://doi.org/10.1103/PhysRevLett.96.076602>
21. Vas, J.V., Thomas, M.J.: Electromagnetic shielding effectiveness of multiwalled carbon nanotube filled silicone rubber. In: *INCEMIC 2015—13th International Conference on Electromagnet Interference and Compatibility Proceeding*, pp. 55–59 (2017). <https://doi.org/10.1109/INCEMIC.2015.8055846>
22. Voelkel, A., Grzeskowiak, T.: The use of solubility parameters in characterization of titanate modified silica gel by inverse gas chromatography. *Chromatographia* **51**, 608–614 (2000). <https://doi.org/10.1007/BF02490820>
23. Mohammadi-Jam, S., Waters, K.E.: Inverse gas chromatography applications: a review. *Adv. Colloid Interface Sci.* **212**, 21–44 (2014). <https://doi.org/10.1016/j.cis.2014.07.002>
24. Voelkel, A.: Inverse gas chromatography in characterization of surface. *Chemom. Intell. Lab. Syst.* **72**, 205–207 (2004). <https://doi.org/10.1016/j.chemolab.2004.01.016>
25. Suarez, I., Caballero, M.J., Coto, B.: A fast and reliable procedure to determine the copolymer composition by GPC-IR: application to ethylene/propylene copolymers and comparison with ¹³C NMR. *Polym. Eng. Sci.* **51**, 317–322 (2011)
26. Suárez, I., Caballero, M.J., Coto, B.: Composition effects on ethylene/propylene copolymers studied by GPC-MALS and GPC-IR. *Eur. Polym. J.* **46**, 42–49 (2010). <https://doi.org/10.1016/j.eurpolymj.2009.09.005>
27. Suárez, I., Caballero, M.J., Coto, B.: Characterization of ethylene/propylene copolymers by means of a GPC-4D technique, *Eur. Polym. J.* **47**, 171–178 (2011). <https://doi.org/10.1016/j.eurpolymj.2010.11.008>